

Magneto-resistive characteristics of the $\text{SrIrO}_3/\text{La}_{2/3}\text{Sr}_{1/3}\text{MnO}_3$ heterostructure

© K.Y. Constantinian¹, G.D. Ulev^{1,2}, A.V. Mashirov¹, A.P. Orlov¹,
I.E. Moskal¹, G.A. Ovsyannikov¹

¹ Kotelnikov Institute of Radio Engineering and Electronics, Russian Academy of Sciences, Moscow, Russia

² Moscow Institute of Physics and Technology (National Research University), Dolgoprudny, Moscow Region, Russia

E-mail: karen@hitech.cplire.ru

Received April 30, 2025

Revised September 8, 2025

Accepted November 11, 2025

We report on results of experimental studies of thin-film heterostructure $\text{SrIrO}_3/\text{La}_{2/3}\text{Sr}_{1/3}\text{MnO}_3$ grown epitaxially on NdGaO_3 substrate. A transitional layer is formed at the interface between paramagnetic semimetal SrIrO_3 , exhibiting strong spin-orbit interaction, and the spin-polarized ferromagnet $\text{La}_{2/3}\text{Sr}_{1/3}\text{MnO}_3$. Single layers of SrIrO_3 and $\text{La}_{2/3}\text{Sr}_{1/3}\text{MnO}_3$ were studied as well. The temperature dependences of electronic conductivity, magnetoresistance, and Hall effect responses obtained at magnetic fields $H = 0-7$ T and temperatures $T = 2-300$ K are discussed.

Keywords: heterostructure, spin-orbit interaction, strontium iridate, manganite, magnetoresistance, Hall effect.

DOI: 10.61011/PSS.2025.12.63114.7787k-25

With the epitaxial growth of oxide films, it becomes possible to create an interface with functional characteristics radically different from those of contacting materials, for example, the formation of a two-dimensional electron gas in a heterostructure with an interface between $\text{LaAlO}_3/\text{SrTiO}_3$ insulators [1]. Recently, heterostructures consisting of magnetics and materials containing metals with high atomic weight and, consequently, with strong spin-orbit coupling (SOC) have attracted increased interest. An anomalous Hall effect was detected [2] in the boundary layer of paramagnetic strontium iridate SrIrO_3 due to the induced magnetic moment from manganite $\text{La}_{2/3}\text{Sr}_{1/3}\text{MnO}_3$. The authors of Ref. [3] reported the occurrence of a Dirac response in SrIrO_3 upon contact with an antiferromagnet SrCuO_2 . The high energy of the SOC SrIrO_3 $E_{SO} \sim 0.5$ eV [4] contributes to the conversion into electric current of the spin current generated by spin pumping during ferromagnetic resonance. Thus, the $\text{SrIrO}_3/\text{La}_{2/3}\text{Sr}_{1/3}\text{MnO}_3$ heterostructure has a spin Hall angle θ_{SH} obtained from the angular dependences of the spin magnetoresistance [5], turned out to be significantly higher than that of structures with a Pt film [6–8]. Considering the prospects of Ir-containing magnetic heterostructures for practical applications of spin-dependent processes, there is a request for a more detailed characterization of the heterostructure of $\text{SrIrO}_3/\text{La}_{2/3}\text{Sr}_{1/3}\text{MnO}_3$ and its forming films in a wide range of temperatures and magnetic fields.

The literature data [9] based on the Hall effect in SrIrO_3 indicate a predominantly electronic type of conductivity, despite the mixed carrier type. In $\text{La}_{2/3}\text{Sr}_{1/3}\text{MnO}_3$ films, the Hall effect and magnetoresistance largely depend on the mismatch of the crystal structure of the film and the sub-

strate [10]. There are also known studies of the temperature dependences of SrIrO_3 films on various substrates [11,12], manganite $\text{La}_{2/3}\text{Sr}_{1/3}\text{MnO}_3$ on SrTiO_3 substrate [13]. This paper provides the results of measurements of the temperature dependences of electrical resistance, magnetoresistance, and Hall response from $\text{La}_{2/3}\text{Sr}_{1/3}\text{MnO}_3$, SrIrO_3 films and the $\text{SrIrO}_3/\text{La}_{2/3}\text{Sr}_{1/3}\text{MnO}_3$ heterostructure on NdGaO_3 substrate when cooled to temperature of $T = 2$ K and magnetic fields up to $H = 7$ T.

Epitaxial thin films of SrIrO_3 and $\text{La}_{2/3}\text{Sr}_{1/3}\text{MnO}_3$ with a thickness of $d = 10-50$ nm were grown on single-crystal substrates (110) NdGaO_3 by radio-frequency magnetron sputtering at a substrate temperature of $770-800^\circ\text{C}$ in a mixture of argon and oxygen gases at a total pressure of $0.3-0.5$ mbar [14,15]. $\text{SrIrO}_3/\text{La}_{2/3}\text{Sr}_{1/3}\text{MnO}_3$ heterostructures were produced by sequential deposition of $\text{La}_{2/3}\text{Sr}_{1/3}\text{MnO}_3$ and SrIrO_3 films in the chamber without vacuum break. The film deposition process was followed by cooling: first rapidly in a sputtering atmosphere of up to 500°C , and then in an oxygen atmosphere at a rate of $10^\circ\text{C}/\text{min}$.

The structural properties of thin-film structures were studied by X-ray diffraction using a Rigaku Smart Lab diffractometer with a rotating copper anode. It followed from the X-ray images [15] that the interplanar spacing in terms of responses (001), (002), (003) and (004) along c -direction from $\text{La}_{2/3}\text{Sr}_{1/3}\text{MnO}_3$ sputtered onto an NdGaO_3 substrate was $\Delta c_{LSMO} = 0.3905 \pm 0.0005$ nm, and for the SrIrO_3 film deposited *in situ* over $\text{La}_{2/3}\text{Sr}_{1/3}\text{MnO}_3$, $\Delta c_{SIO} = 0.404 \pm 0.001$ nm. From a cross-section image of a heterostructure on a Thermo Fisher Titan Themis Z trans-

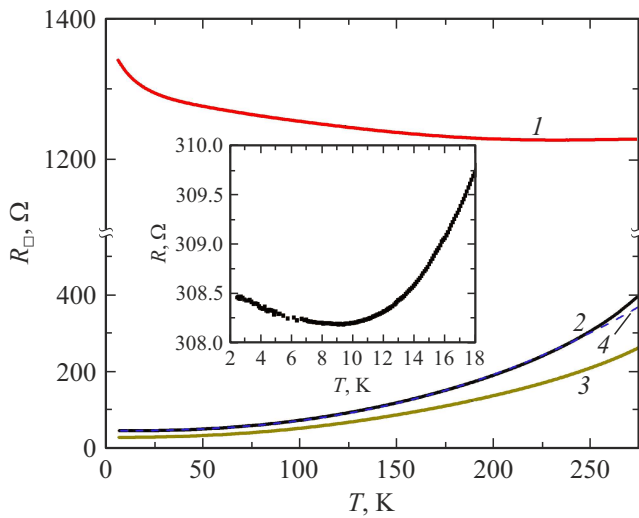


Figure 1. Temperature dependences of resistance per square (R_{\square}) of individual films and heterostructure: SrIrO₃ (1), La_{2/3}Sr_{1/3}MnO₃ (2), SrIrO₃/La_{2/3}Sr_{1/3}MnO₃ (3). The dotted line (4) shows an approximation by a power function $\propto T^{5/2}$ of the temperature dependence of the resistance of $L = 0.65$ mm long La_{2/3}Sr_{1/3}MnO₃ film. Insert — low-temperature section $R(T)$ La_{2/3}Sr_{1/3}MnO₃.

mission electron microscope, visualizing the interface between SrIrO₃, La_{2/3}Sr_{1/3}MnO₃ films and the NdGaO₃ substrate, it followed that the films are grown with an epitaxial ratio (001)SrIrO₃//(001)La_{2/3}Sr_{1/3}MnO₃//(110)NdGaO₃, [001]SrIrO₃//[001]La_{2/3}Sr_{1/3}MnO₃//[001]NdGaO₃.

The electrophysical characteristics of the films and the heterostructure were studied using a 4-point measurement scheme with the „Hall“ cross geometry with a width of $W = 100 \mu\text{m}$ and a length of $L = 0.65$ mm. Metallized contact pads on the heterostructure were placed on top of the SrIrO₃ film. The Hall effect response and magnetic resistance voltages were measured at a temperature of $T = 2\text{--}300$ K in a cryostat with a superconducting solenoid in a magnetic field from H to ± 7 according to the method [16], which minimizes the effect of thermoelectrical effects by switching the polarity of the set measuring current I with a switching frequency set by the pulse duration (usually on the order of 1.5 s). The response voltage was recorded with a Keithley 2600B nanovoltmeter, and the temperature on the sample was recorded using a Lake Shore Cernox sensor.

Figure 1 shows the temperature dependences of the resistance of $R_{\square}(T) = R(T) \cdot W/L$ at $H = 0$ of SrIrO₃ films with $d_{\text{SIO}} = 35$ nm, La_{2/3}Sr_{1/3}MnO₃ with $d_{\text{LSMO}} = 40$ nm and heterostructure with $d_{\text{SIO/LSMO}} = 35$ nm ($d_{\text{SIO}} = 10$ nm, $d_{\text{LSMO}} = 25$ nm). It is possible to see the difference between $R_{\square}(T)$ for SrIrO₃ and La_{2/3}Sr_{1/3}MnO₃ films, whose shunting role is manifested on $R_{\square}(T)$ of heterostructure. In the region of relatively high temperatures of $T = 50\text{--}250$ K the dependence $R_{\square}(T)$ of the La_{2/3}Sr_{1/3}MnO₃ film is well described by the power law $R(T) \propto T^{5/2}$ as in

ferromagnetic half-metals [17]. An inflection of $R(T)$ occurs in the low temperature range of $T < 20$ K on $T_{\text{min}} = 9.5$ K at $R_{\square}(T)$ La_{2/3}Sr_{1/3}MnO₃ (inset in Figure 1), interpreted by weak localization in the three-dimensional case [18] with a root dependence of the specific conductivity $\Delta\sigma = \sigma - \sigma_0 \sim a \cdot (t)^{1/2}$, where $\sigma_0 = \sigma(T = 0)$, $t = T/T_{\text{min}}$, a is the proportionality coefficient. The experimental dependences $R_{\square}(T)$ are conveniently approximated by the functions of the normalized resistivity $\Delta\rho = (\rho - \rho_{\text{min}})/\rho_{\text{min}}$, where $\rho = R_{\square} \cdot d$, $\rho_{\text{min}} = \rho(T_{\text{min}})$.

Figure 2 shows the experimental dependences of the normalized resistivity for La_{2/3}Sr_{1/3}MnO₃ and the heterostructure at $T < 20$ K and approximations of the form $b\rho(t)^{5/2} + (a(t)^{1/2} + \sigma_0)^{-1}$. In the case of film La_{2/3}Sr_{1/3}MnO₃ $\rho_{\text{min}} = 1.9 \cdot 10^{-4} \Omega \cdot \text{cm}$, $T_{\text{min}} = 9.6$ K; in the heterostructure SrIrO₃/La_{2/3}Sr_{1/3}MnO₃ $\rho_{\text{min}} = 1.0 \cdot 10^{-4} \Omega \cdot \text{cm}$, $T_{\text{min}} = 8.7$ K. At the same time, $R_{\text{min}} = 308.2 \Omega$ for La_{2/3}Sr_{1/3}MnO₃ and the heterostructure $R_{\text{min}} = 196.4 \Omega$ with the same (within the error ± 0.5 nm)

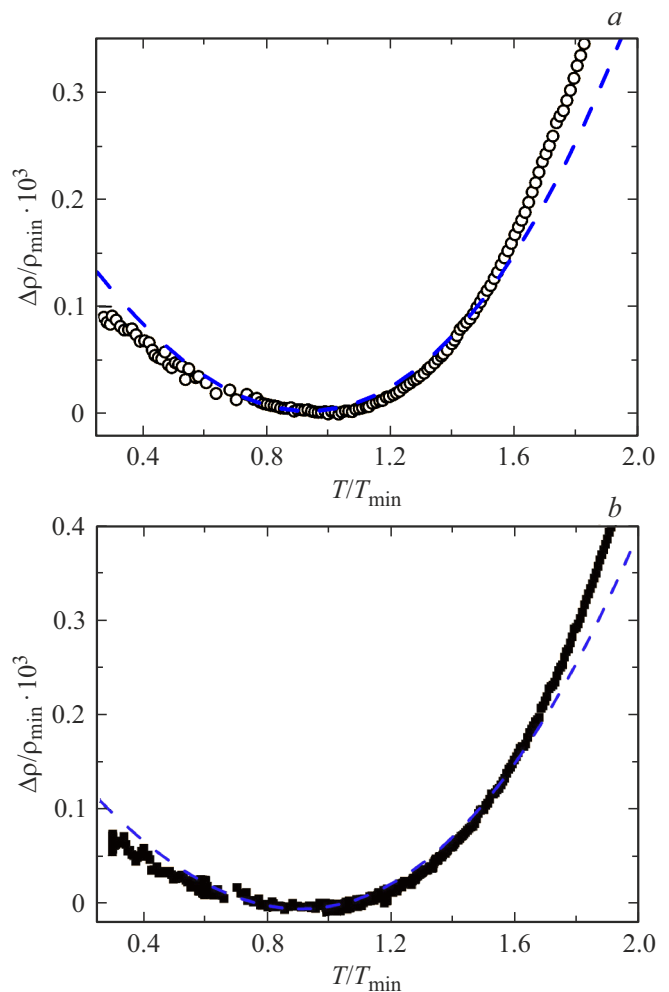


Figure 2. Normalized temperature dependences of the difference of the resistivity $\Delta\rho(t)/\rho_{\text{min}}$: La_{2/3}Sr_{1/3}MnO₃ film (a), SrIrO₃/La_{2/3}Sr_{1/3}MnO₃ heterostructure (b). The dashed lines show the approximation dependencies.

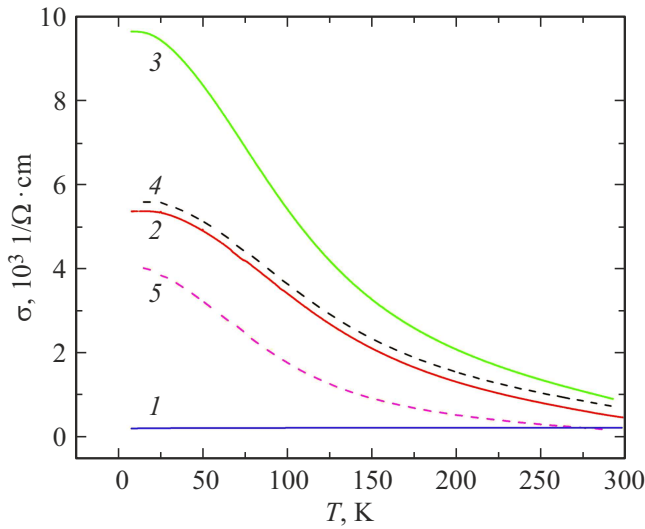


Figure 3. Experimental temperature dependences at $H = 0$ of the specific conductivities of films and heterostructures: 1 — $\sigma_1(T)$ $d_{\text{SIO}} = 35$ nm, 2 — $\sigma_2(T)$ $d_{\text{LSMO}} = 40$ nm, 3 — $\sigma_3(T)$ $d_{\text{SIO/LSMO}} = 35$ nm. Dashed lines: 4 — $\sigma_4(T) = \sigma_1(T) + \sigma_2(T)$, 5 — $\sigma_5(T) = \sigma_3(T) - \sigma_4(T)$.

thickness $d_{\text{SIO}} = d_{\text{SIO/LSMO}}$. It should be noted that the relative accuracy of the definition of $\Delta\rho/\rho_{\text{min}}$ was at least 5 characters. Weak localization in thin films of manganite with a inflection $R(T)$ at low temperatures of $T < 20$ K was reported in Refs. [13,19].

Figure 3 shows the temperature dependences of the specific conductivities $\sigma_i(T)$ of individual films and the heterostructure: $i = 1$ (SrIrO₃), $i = 2$ (La_{2/3}Sr_{1/3}MnO₃), $i = 3$ (SrIrO₃/La_{2/3}Sr_{1/3}MnO₃). As can be seen, the trivial summation of $\sigma_4(T) = \sigma_1(T) + \sigma_2(T)$ differs markedly from the $\sigma_3(T)$ of heterostructure. The figure also shows the difference curve 5, corresponding to the contribution from the transition layer $\sigma_5(T) = \sigma_3(T) - \sigma_4(T)$. The formation of an intermediate layer at the SrIrO₃/La_{2/3}Sr_{1/3}MnO₃ boundary was reported in Ref. [2], but its resistive parameters were not discussed.

A Hall-cross configuration was used to measure magnetoresistance and Hall response. The longitudinal current I_{xx} was set and the voltage dependences on the magnetic field were measured: transverse $V_{xy}(H)$ and longitudinal $V_{xx}(H)$. In the case of the heterostructure, the upper SrIrO₃ film was used to set the current I_{xx} and measure the voltages V_{xx} and V_{xy} . The magnetic field H was directed perpendicular to the film plane and ranged from 0 to $H_{\text{max}} = 7$ T. Due to the change in the polarity of the current I_H supplied to the solenoid, the direction of the magnetic field changed.

It should be noted that the Hall responses in manganites are ambiguously dependent on temperature, in particular, in Refs. [10,20] it was reported that both a change in the sign of the Hall resistance and a response from the anomalous Hall effect were observed in the experiment. Figure 4 shows the dependences of the Hall voltage

and magnetoresistance at $T \sim 10$ K, when the electrical conductivity La_{2/3}Sr_{1/3}MnO₃ can be considered metallic, and the Hall response $V_{xy}(H)$ demonstrates growth with a field H and negative magnetoresistance.

It can be seen from figure 4a that the voltages V_{xy} for all three samples linearly depend on the field H and the Hall resistance $R_H = V_{xy}d_i/\mu_0H$ with a simplified estimate of the effective carrier concentration $n_{\text{eff}} = 1/eR_H$ (μ_0 and e — physical constants) for $T = 10$ K, we obtain for La_{2/3}Sr_{1/3}MnO₃ a hole $n_{\text{eff}} = 1.6 \cdot 10^{22} \text{ cm}^{-3}$, and for SrIrO₃ and SrIrO₃/La_{2/3}Sr_{1/3}MnO₃ electronic n_{eff} : $1.4 \cdot 10^{21} \text{ cm}^{-3}$ and $1.25 \cdot 10^{22} \text{ cm}^{-3}$ respectively. It should be noted that the parameters of mobility (μ_e, μ_h) and concentration (n_e, n_h) of electrons and holes in thin SrIrO₃ films on the SrTiO₃ substrate were taken into account separately in Ref. [9]. The mobility ratio $\mu_e/\mu_h \sim 0.3$ was reported for La_{2/3}Sr_{1/3}MnO₃ films in Ref. [10], indicating a

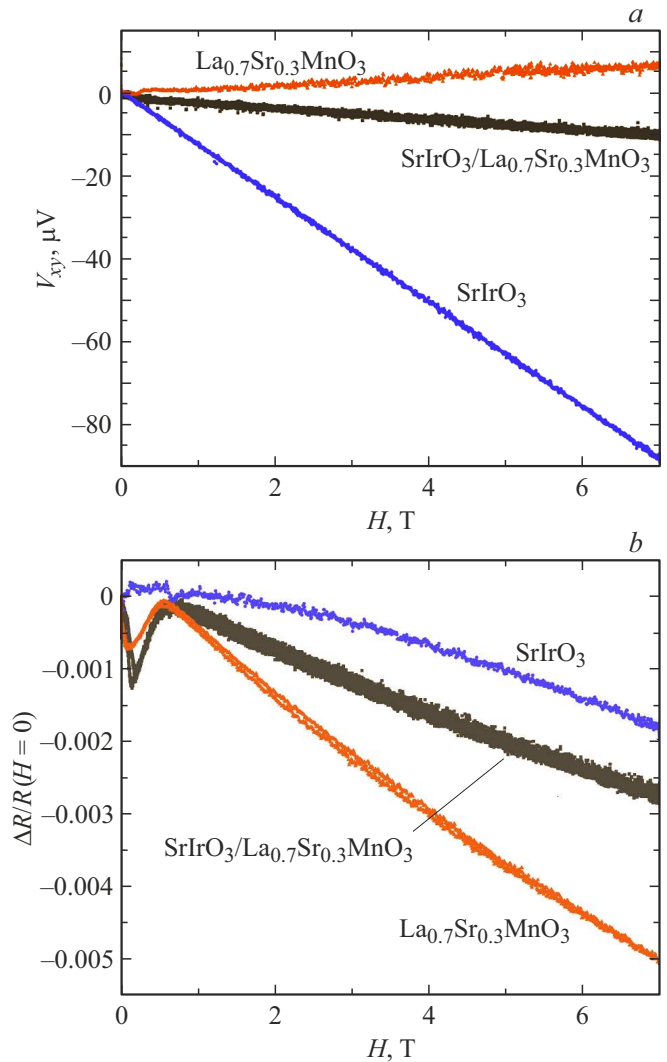


Figure 4. Dependences of Hall voltage (a) and magnetic resistance (b) SrIrO₃, La_{2/3}Sr_{1/3}MnO₃ and SrIrO₃/La_{2/3}Sr_{1/3}MnO₃ at $T = 10$ K. The amplitude of the alternating measuring current $I_{xx} = 100 \mu\text{A}$.

difference in the effective masses of electrons and holes in these materials.

Figure 4b shows the dependences of the resistance drop normalized by $R(0)$ $\Delta R = R(H) - R(0)$ on the magnetic field H . It can be seen that the SrIrO₃ film has a negative magnetic resistance over the entire range of fields H . Negative magnetoresistance in La_{2/3}Sr_{1/3}MnO₃ film and SrIrO₃/La_{2/3}Sr_{1/3}MnO₃ heterostructure occurs at $H > 1$ T, however, in the field interval of $H = 0-1$ T, the sign of $\Delta R(H)/R(0)$ changes twice on La_{2/3}Sr_{1/3}MnO₃ and on SrIrO₃/La_{2/3}Sr_{1/3}MnO₃. The repeatability should be noted — figure 4b shows well-matching double tracks of magnetoresistance recording. A similar change in the sign of the magnetoresistance was reported in Ref. [21] for the ferromagnetic superlattice SrRuO₃/La_{2/3}Sr_{1/3}MnO₃. The authors of Ref. [21] attribute the appearance of a positive sign of magnetoresistance to weak antilocalization due to SOC, which manifests itself when varying the thicknesses of ferromagnets in the superlattice and magnetic anisotropy due to layers of SrRuO₃ in a superlattice grown on SrTiO₃. In our case, the positive sign of $\Delta R(H)/R(0)$ in the range of $H = 1.1-5.5$ kOe on La_{2/3}Sr_{1/3}MnO₃ film grown on NdGaO₃ substrate is difficult to bind with weak antilocalization, and covering La_{2/3}Sr_{1/3}MnO₃ with SrIrO₃ film with strong SOC, on the contrary, only reduced the difference $\Delta R(H)/R(0)$ approximately by 1.5 times. Almost the same ratio of 1.57 is obtained for values R_{\min} for La_{2/3}Sr_{1/3}MnO₃ film and heterostructure.

Eventually, temperature dependences are obtained at $T = 2-300$ K of the electrical conductivity of thin films of SrIrO₃, La_{2/3}Sr_{1/3}MnO₃ and SrIrO₃ heterostructure on the NdGaO₃ substrate. From Hall measurements at $T = 10$ K and $H < 7$ T, it was found that SrIrO₃ exhibits an electronic type of conductivity and negative magnetoresistance. The film of ferromagnetic Half-metal La_{2/3}Sr_{1/3}MnO₃ has hole-like conductivity under the same experimental conditions, and the magnetic resistance at $H < 1$ T changes sign twice from negative to positive and vice versa, the same happens for the SrIrO₃/La_{2/3}Sr_{1/3}MnO₃ heterostructure. A drop in resistance with a minimum of $T \sim 10$ K is found at $T < 15$ K on La_{2/3}Sr_{1/3}MnO₃ and SrIrO₃/La_{2/3}Sr_{1/3}MnO₃ which is described by weak localization in the three-dimensional approximation.

Acknowledgments

The authors are grateful to V.A. Baidikova, Yu.V. Kislinsky, A.V. Shadrin and A.M. Petrzhik for sample fabrication and useful comments.

Funding

This study was supported by grant No. 23-79-00010 by the Russian Science Foundation.

Conflict of interest

The authors declare no conflict of interest.

References

- [1] S. Chen, Y. Ning, C. Tang, L. Dai, S. Zeng, K. Han, J. Zhou, M. Yang, Y. Guo, C. Cai, A. Ariando, A.T.S. Wee, X. Yin. *Adv. Electron. Mater.* **10**, 2300730 (2024). DOI: 10.1002/aelm.202300730
- [2] M. Yoo, J. Tornos, A. Sander, L. Lin, N. Mohanta, A. Peralta, D. Sanchez-Manzano, F. Gallego, D. Haskel, J.W. Freeland, D.J. Keavney, Y. Choi, J. Stremper, X. Wang, M. Cabero, H.B. Vasili, M. Valvidares, G. Sanchez-Santolino, J.M. Gonzalez-Calbet, A. Rivera, C. Leon, S. Rosenkranz, M. Bibes, A. Barthelemy, A. Anane, E. Dagotto, S. Okamoto, S.G.E. te Velthuis, J. Santamaria, J.E. Villegas. *Nat. Comm.* **12**, 3283 (2021). DOI: 10.1038/s41467-021-23489
- [3] S. Jana, T. Senapati, S.G. Bhat, S.N. Sarangi, K. Senapati, D. Samal. *Phys. Rev. B* **107**, 134415 (2023). DOI: 10.1103/PhysRevB.107.134415
- [4] G. Cao, P. Schlottmann. *Rep. Progress in Phys.* **81**, 042502 (2018). DOI: 10.1088/1361-6633/aaa979
- [5] G.A. Ovsyannikov, K.I. Konstantinyan, G.D. Ul'ev, I.E. Moskal. *JETP Lett.* **121**, 5, 381, (2025). DOI: 10.1134/S002136402560017X
- [6] T. Nan, S. Emori, C.T. Boone, X. Wang, T.M. Oxholm, J.G. Jones, B.M. Howe, G.J. Brown, N.X. Sun. *Phys. Rev. B* **91**, 214416 (2015). DOI: 10.1103/PhysRevB.91.214416
- [7] G.D. Ulev, K.Y. Constantinian, I.E. Moskal', G.A. Ovsyannikov, A.V. Shadrin. *J. Commun. Technol. Electronics* **68**, 10, 1201 (2023). DOI: 10.1134/S1064226923100194
- [8] Y.-T. Chen, S. Takahashi, H. Nakayama, M. Althammer, S.T.B. Goennenwein, E. Saitoh, G.E.W. Bauer. *J. Phys. D: Condens. Matter* **28**, 103004 (2016). DOI: 10.1088/0953-8984/28/10/103004
- [9] N. Manca, D.J. Groenendijk, I. Pallecchi, C. Autieri, L.M.K. Tang, F. Telesio, G. Mattoni, A. McCollam, S. Picozzi, A.D. Caviglia. *Phys. Rev. B* **97**, 081105(R) (2018). DOI: 10.1103/PhysRevB.97.081105
- [10] I.M. Dildar, C. Beckman, X. He, J. Aarts. *Phys. Rev. B* **85**, 205103 (2012). DOI: 10.1103/PhysRevB.85.205103
- [11] F.-X. Wu, J. Zhou, L.Y. Zhang, Y.B. Chen, S. Zhang, Z. Gu, S. Yao, Y. Chen. *J. Phys.: Condens. Matter* **25**, 125604 (2013). DOI: 10.1088/0953-8984/25/12/125604
- [12] A. Biswas, Y.H. Jeong. *Current Appl. Phys.* **17**, 605–614 (2017). DOI: 10.1016/j.cap.2016.09.020
- [13] L.E. Calvet, G. Agnus, P. Lecoeur. *J. Vac. Sci. Technol. A* **37**, 031504 (2019). DOI: 10.1116/1.5085669
- [14] I.E. Moskal, A.M. Petrzhik, Y.V. Kislinskii, A.V. Shadrin, G.A. Ovsyannikov, N.V. Dubitskiy. *Bulletin RAS: Physics*, **88**, 4, 582–585 (2024). DOI: 10.1134/S1062873823706360
- [15] G.A. Ovsyannikov, K.Y. Constantinian, V.A. Shmakov, A.L. Klimov, E.A. Kalachev, A.V. Shadrin, N.V. Andreev, F.O. Milovich, A.P. Orlov, P.V. Lega. *Phys. Rev. B* **107**, 144419 (2023). DOI: 10.1103/PhysRevB.107.144419
- [16] J. Lindemuth. *Hall Effect Measurement Handbook: A Fundamental Tool for Semiconductor Material Characterization.* (Lake Shore Cryotronics, Inc. 2020).

- [17] X. Wang, X.-G. Zhang. Phys. Rev. Lett. **82**, 21, 4276 (1999). DOI: 10.1103/PhysRevLett.82.4276
- [18] P.A. Lee, T.V. Ramakrishnan. Phys. Rev. B **26**, 4008 (1982).
- [19] W. Niu, M. Gao, X. Wang, F. Song, J. Du, X. Wang, Y. Xu, R. Zhang. Sci. Reports **6**, 26081 (2016). DOI: 10.1038/srep26081
- [20] Y. Lyanda-Geller, S.H. Chun, M.B. Salamon, P.M. Goldbart, P.D. Han, Y. Tomioka, A. Asamitsu, Y. Tokura. Phys. Rev. B **63**, 184426 (2001). DOI: 10.1103/PhysRevB.63.184426
- [21] R.S. Helen, W. Prellier, P. Padhan. J. Appl. Phys. **128**, 033906 (2020). DOI: 10.1063/5.0014909

Translated by A.Akhtyamov